Bull. Res. Inst. Mar. Sci. & Tech,
Korea Maritime University,
Vol. 1. No. 1, p. 71-84.

The Korean Journal of Quaternary Research
Vol. 5, No. 1, 33~46 (1991)

Sandy Sediment Transport Mechanism on Tidal Sand Bodies, West Coast of Korea

Yong Ahn Park, Hyo Jin Kang* and Y. I. Song**
Department of Oceanorgraphy, Seoul National University, Seoul 151-742, Korea
* Department of Ocean Engineering, Korea Maritime University, Pusan 606-791, Korea
**Department of Oceanography, Korea Navy Academy, Jinhae, Korea

해양(조수환경) 사립퇴적물의 이동기작에 관한 연구 — 한국 서해 만경강·동진강 하구 해역 —

박 용 안·강 효 진*·송 영 일**
서울대학교 해양학과 *한국해양대학교 해양공학과 **해군사관학교 해양학과

ABSTRACT

Sand bars associated with strong tidal currents are well developed in the subtidal zone near the Kokunsan islands. Tidal currents measured at sand bar in the area show an asymmetry in magnitude between flood and ebb currents. At the southern flank of the sand bar the currents are flood-dominant whereas the currents are ebb-dominant at the northern flank. The asymmetry is more distinctive as the currents become stronger during spring tide. Moreover, the flood-dominance along the southern flank is stronger than the ebb-dominance along the northern flank. Thus the flood current is more affective to the sand bar. The sandy bottom sediment is mostly transported as bedload by the tidal currents. The magnitude asymmetry of the tidal currents results in a net sediment movement in one direction. The direction is onshore in the south and offshore in the north, which may result in a net counterlookwise rotation of the sands around the sand bar. However, the sand bar may migrate towards onshore due to the more affective flood current in the south. The irregular V-shaped outline of the sand bar in the south also seem to reflect the strong effect of flood current.

요 약

조류가 강한 만경강-동진강 부근의 연안역에는 많은 사주들이 잘 발달하여

The present study was supported by the academic research funding program, Ministry of Education, 1989.

있다. 그 중 한 사주에서 측정된 조류는 그 최대유속이 밀물과 썰물 사이에 심한 비대칭 현상을 나타낸다. 사주의 남쪽 측면에서는 밀물이 우세하고 북쪽 측면에서는 썰물이 우세한 이러한 비대칭성은 대조시 유속이 강할 때 더욱 뚜렷이 나타난다. 또한 남쪽의 밀물 우세 현상은 북쪽의 썰물 우세 현상 보다 더욱 강하게 나타나고 있어 사주는 전체적으로 밀물에 의하여 더 큰 영향을 받고 있다. 모래로 이루어진 이 지역의 해저 퇴적물들은 대부분 조류에 의해 밑짐으로 이동 되고 있으며, 이러한 조류의 비대칭성으로 인하여 모래는 어느 한 방향으로 순 이동이 일어나게 된다. 이러한 모래의 순 이동은 남쪽에서는 해안쪽으로 북쪽에서는 외해쪽으로 이동하여 바닥의 모래는 사주를 반시계 방향으로 순환하는 양상을 띄게 될 것이며 전체적으로는 강한 밀물의 영향으로 사주가 해안쪽으로 이동하는 결과를 가능하게 할 것이다. 사주의 남쪽부분의 형태가 불규칙적이고 V자 모양을 나타내는 것도 이러한 강한 밀물의 영향을 반영하는 것으로 해석된다.

INTRODUCTION

Pattern of sediment transport in coastal region is largely affected by waves and currents which are easily modified by the bedforms. Cohesionless coarse sediments are usually transported as bedload by the tractive force exerted by the flow acting on the grain near the bottom (Komar, 1978; Sleath, 1984), and the movement of sediment by traction results in various bedforms of different shapes and sizes (Bagnold, 1946; Holman and Bowen, 1982; Stride et al., 1982). The various bedforms in turn deform and distort the flow condition which changes the bedforms again, sometimes resulting in the migration of bedforms (Ludwick, 1972; 1975).

In the coastal region, where tidal currents are strong and abundant sand material is available, large sand bars are well developed (Off, 1963; Caston, 1972; Jordan, 1972; Belderson et al., 1982; Stride et al., 1982). Due to the big volume of the sand bars sediment movement on the sand bars together with the bedform migration plays an important role in the sediment budget of the coastal area (Caston, 1981).

The present study investigates the mechanism and transport pattern of surface sediment on sand bar in relation to the sediment characteristics and tidal current. One of the sand bars near the Kokunsan Islands was selected (Fig. 1). Data from grab samples at ten locations and tidal current measurement at two stations were analyzed (Fig. 2). Delineation of the sand bank was done by using the nautical chart (Hydrographic Office of Korea, 1989) together with the visual observation during the low tide when the surface of the sand bar was exposed. Water samples at the surface and 1 m above the bottom were also collected for the analysis of suspended sediment content.

STUDY AREA AND SAND BAR

The study area is located at the mouth of the Keum and Mangyung Rivers. Due to the high tidal range reaching up to 6 m and the strong tidal currents up to 2-3 knots (Hydrographic Office of Korea, 1990) numerous sand bodies separated by major tidal channels develop, which trend of east-west or northeast-southwest (Fig. 1). Tidal channels are mostly 10-15 km wide. Maximum depth of the four major channels reached up to 26 m. The sediment bodies separated by the channels are mostly linear sand bars or banner sand bars (Jordan, 1962; Off, 1963; Caston, 1972; Belderson et al., 1982). Abundant input of clastic sediments from the Keum and Mangyung Rivers (Lee and Chough, 1989) and strong tidal current make the

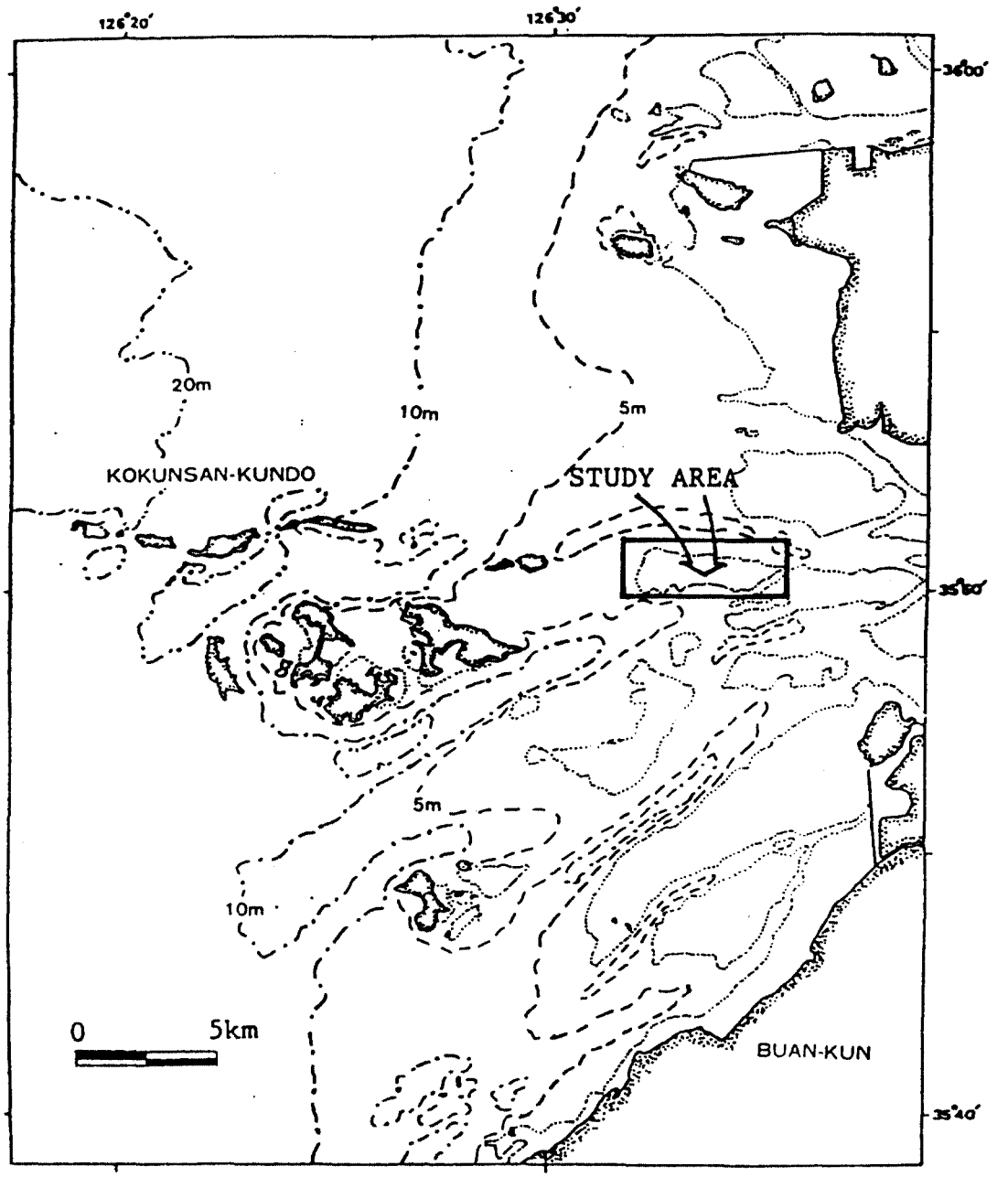

Figure 1. Map showing the study area

area a favorable region for the development of sand bars.

Sand bars or banks in the study area are mostly linear except for the banner sand bars which develop behind the islands (Fig. 1). The sand bars are generally 4-15 km long and 1-4 km wide. The top of the sand bars are flat with various forms of ripple marks. They are submerged during the high tide and exposed during the low tide. The long axes of the linear sand bars in the study area are slightly oblique with an angle of 0-20 degrees to the direction of the strong tidal currents (Fig. 1).

The sand bar for the present study shows a

nearly straight outline in the north whereas the outline in the south is irregular showing a V-shape in general. The surface of the sand bar is also out by a shallow tidal channel (Fig. 2). The long axis of the sand bar trends approximately 20 degrees clockwise to the major direction of tidal currents. Slope of the flanks on either side of the long axis is generally steeper in the north side than in the south side. Top of the sand bar is flat and ripple marks of various size and shape occur on the surface. The size of ripples are generally 5-10 cm in wavelength, 3-5 cm in wave height, and the crest length is 10-20 cm. Several megaripples were also found on the southern flank. The megaripples were approximately 0.5 m high and 5-10 m long with the crest lenghth of about 30-50 m. The crest line of the megaripples was usually perpendicular to the long axis of the sand bar.

Surface sediment of the sand bar is mostly comprised of moderately to well sorted, fine to very fine sand containing little silt or clay (Table

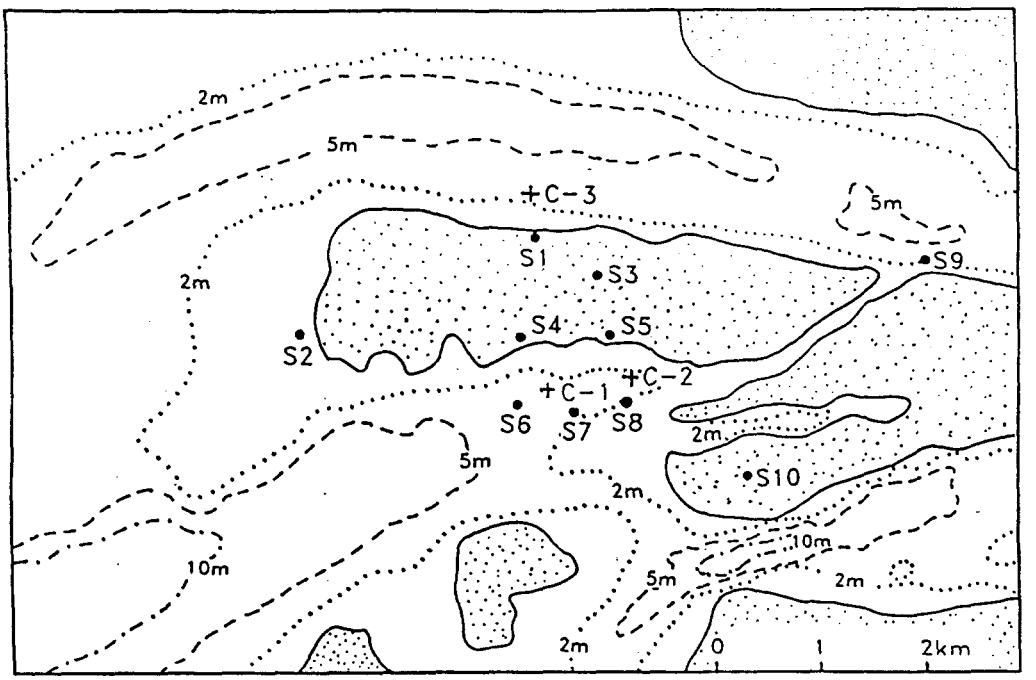

Figure 2. Map showing the sand bar and the associated tidal channels, stations for the surface sediment sample (S1-S10), current measurement during the average tide (C-1), and current measurement and water samples during the spring tide (C-2, C-3).

Table 1. Grain size characteristics around the sand bar

St.	Sand (%)	Silt (%)	Clay (%)	Mean (phi)	Sorting (phi)
S1	92.2	4.4	3.4	3.38	0.51
S2	90.4	4.6	5.0	4.10	1.10
S4	96.5	2.1	1.4	2.96	0.56
S5	96.8	1.5	1.7	3.07	0.47
S6	3.3	4.2	2.5	3.00	0.70
S7	93.4	3.4	1.2	3.45	0.41
S8	96.1	2.0	1.9	3.14	0.46
S9	92.7	3.6	3.7	3.18	0.58
S10	55.7	31.6	12.7	4.64	1.98

1). The surface sediment of the sand bar does not show any distinctive trend except that the sediment of the central part of the sand bar looks slightly coarser than the other areas. Suspended sediment content in the water column was highly variable with time and depth reaching more than 200 mg/l during the maximum flood current near the bottom. Generally the content was higher in the south and near the bottom. However most of the sediment filtered was finer than 64 μm.

TIDAL CURRENTS AND VELOCITY ASYMMETRY

Tidal currents in the study area flow mostly northeast-southwest with the maximum speed of about 2 knots (Hydrographic Office of Korea, 1990). However, this general trend of tidal currents changes significantly according to the regional geomorphology resulting in an asymmetry in duration and speed between flood and

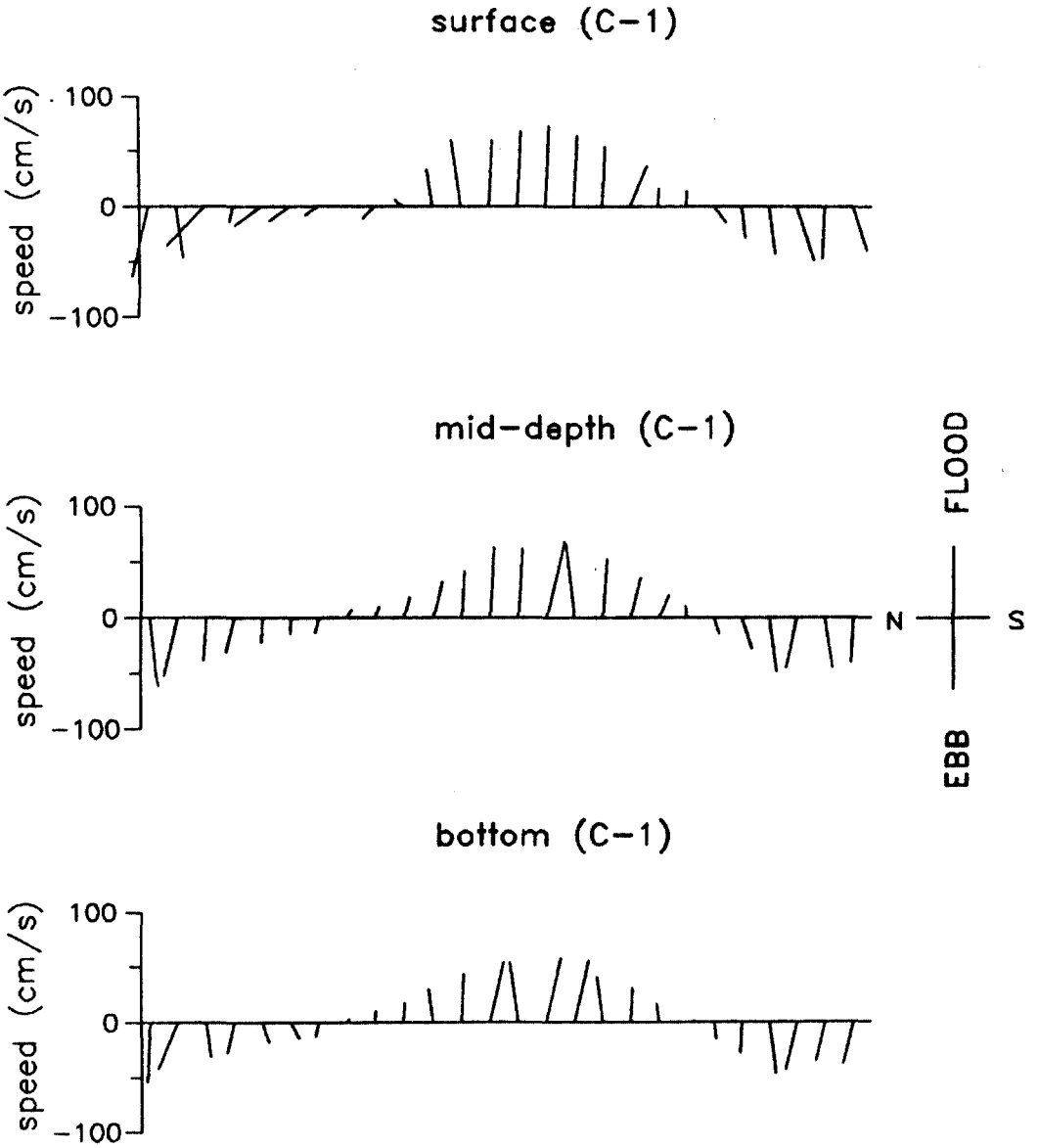

Figure 3. Current speed and direction with time in the south (C-1) during the average tide.

ebb currents (Huthnance, 1973; Howarth, 1982).

At a station near the southern flank of the sand bar (Station C-1) current measurement was done every half hour by using a direct reading current meter for 13 hours when the tide of the day was approximately a week after the spring tide. The measurement was done by 1 m interval form the surface to the bottom. About a month later during a spring tide currents at the northern side and the southern side (Stations C-2 and C-3) were measured at the same time by the same method for the Station C-1 using two current meters.

At the southern station (St. C-1) when the tidal range was approximately average of spring and neap tides, the tidal currents show a weak flood-dominant asymmetry in magnitude. Maximum current speed at the surface was 74.0 cm/sec for the flood and 65.6 cm/sec for the ebb. The durations for the flood and ebb were about

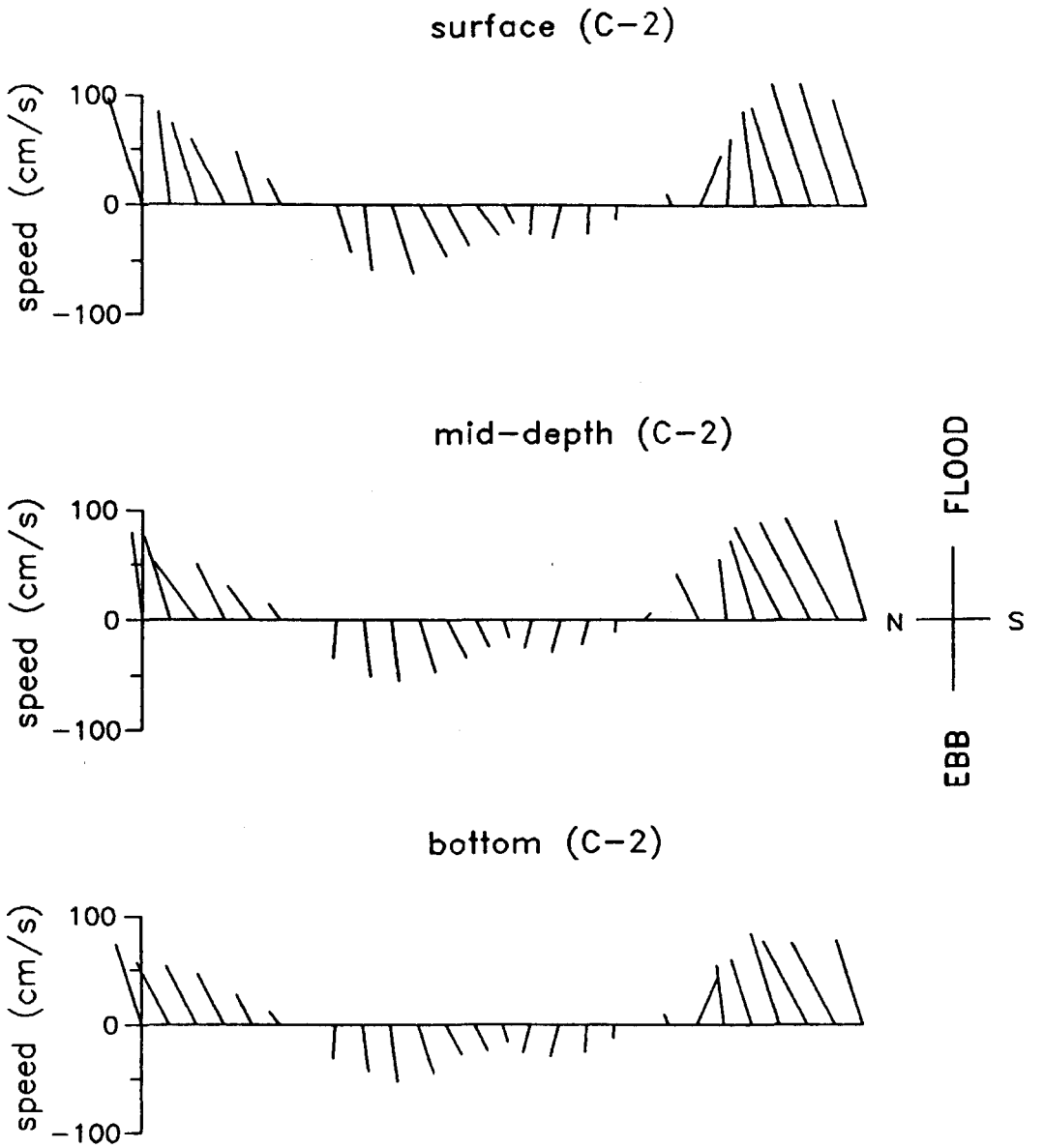

Figure 4. Current speed and direction with time in the south (C-2) during the spring tide.

the same. This weak flood dominance is also shown throughout the depth. Velocity gradient from the surface to the bottom is great when the surface current is greater than approximately 1 knot (Fig. 3). However when the tidal currents are strong during the spring tide the flood dominance in magnitude is extremely enhanced at the southern station (St. C-2). At the surface water, maximum flood speed was 117.0 cm/sec whereas the maximum ebb speed was 51.8 cm/sec which was even smaller than the maximum ebb during the average tide. Durations for the flood and ebb do not show a significant difference each other. Maximum velocity gradient with depth is shown during the maximum flood, which suggests a stronger shear stress at the bottom during the maximum flood current (Fig. 4).

At the northern station (St. C-3), currents measured at the same time with the southern station (St. C-2) during the spring tide show a strong ebb-dominant asymmetrical pattern in

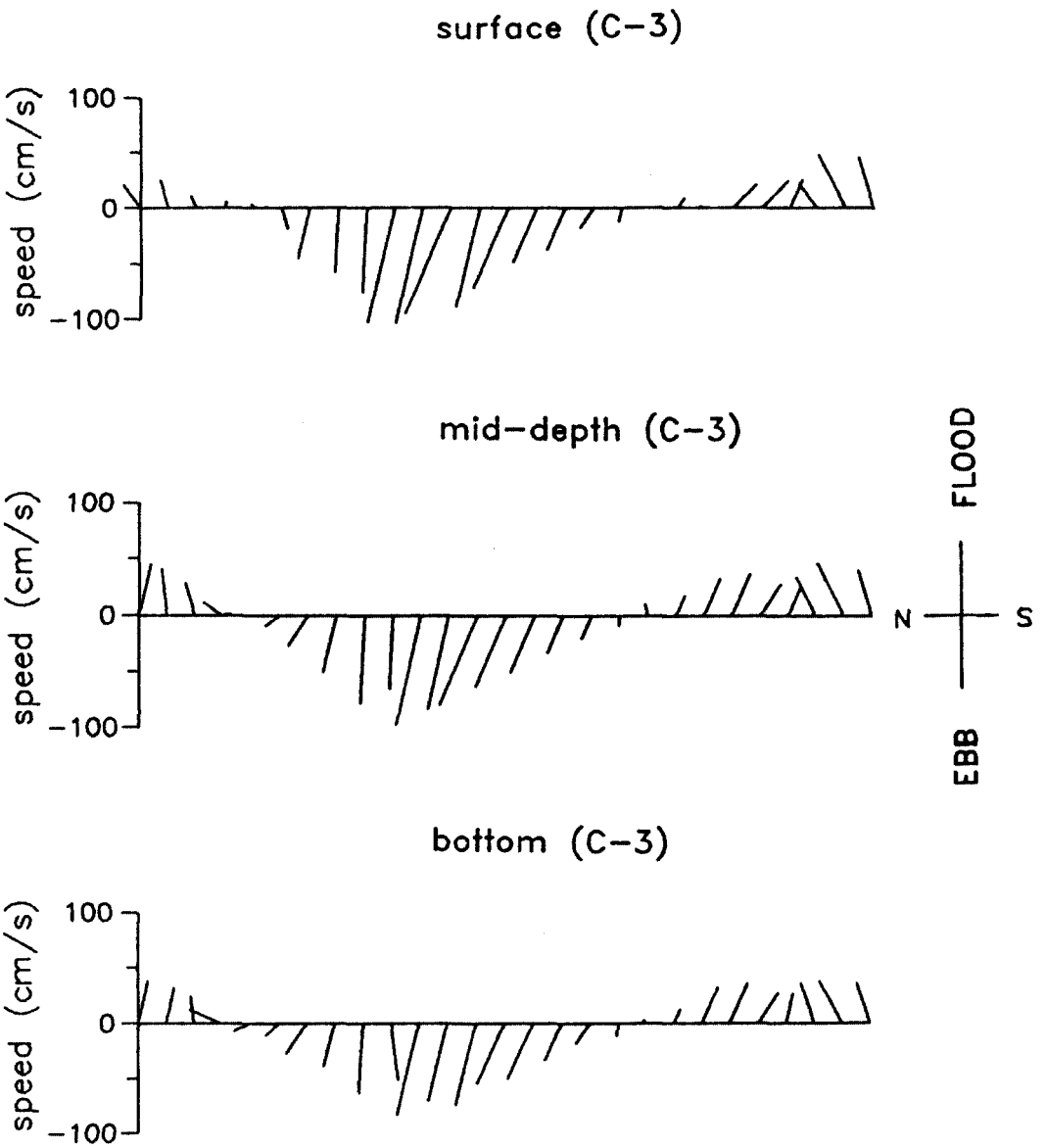

Figure 5. Current speed and direction with time in the north (C-3) during the spring tide.

Table 2. Speed and direction of the residual current: cm/sec (degree)

St.	Surface	Mid-depth	Bottom
C-1	2.79 (51)	2.35 (139)	0.12 (110)
C-2	8.53 (78)	21.08 (59)	17.91 (62)
C-3	6.00 (295)	13.08 (311)	10.65 (307)

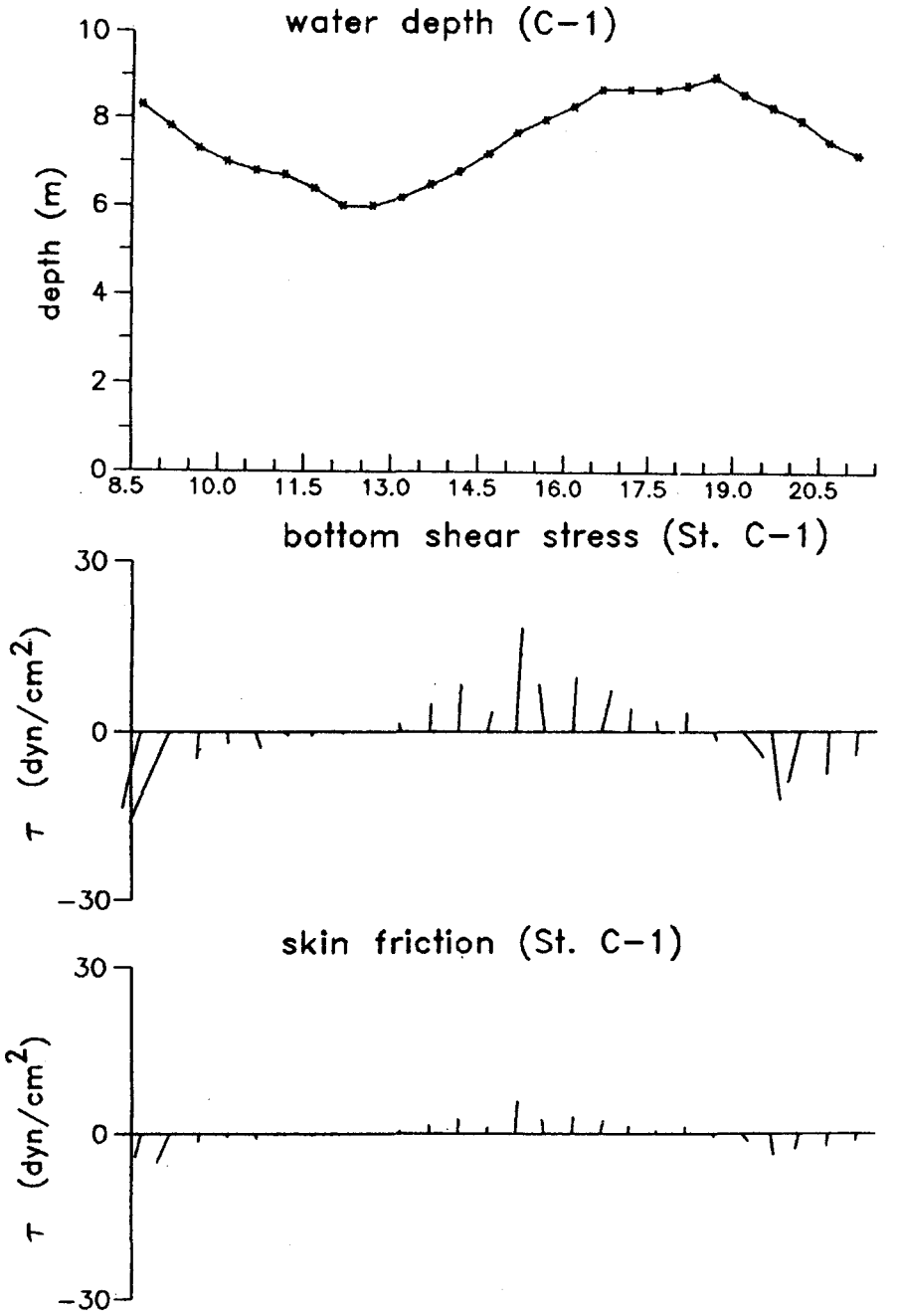

Figure 6. Bottom shear stress and skin friction in the south (C-1) during the average tide.

magnitude. The maximum flood speed was 55.1 cm/sec while the maximum ebb speed was 106.1 cm/sec at the surface. However the difference between maximum flood and ebb is smaller than the difference at the southern station. Weak ebb dominant duration asymmetry is also found. Maximum vertical velocity gradient appears during the maximum ebb current. Direction of currents are slightly deviated toward SEE-NWW from the general current direction of the area and the direction during the flood is somewhat variable compared to the consistent strong ebb current (Fig. 5).

The asymmetrical pattern of the currents

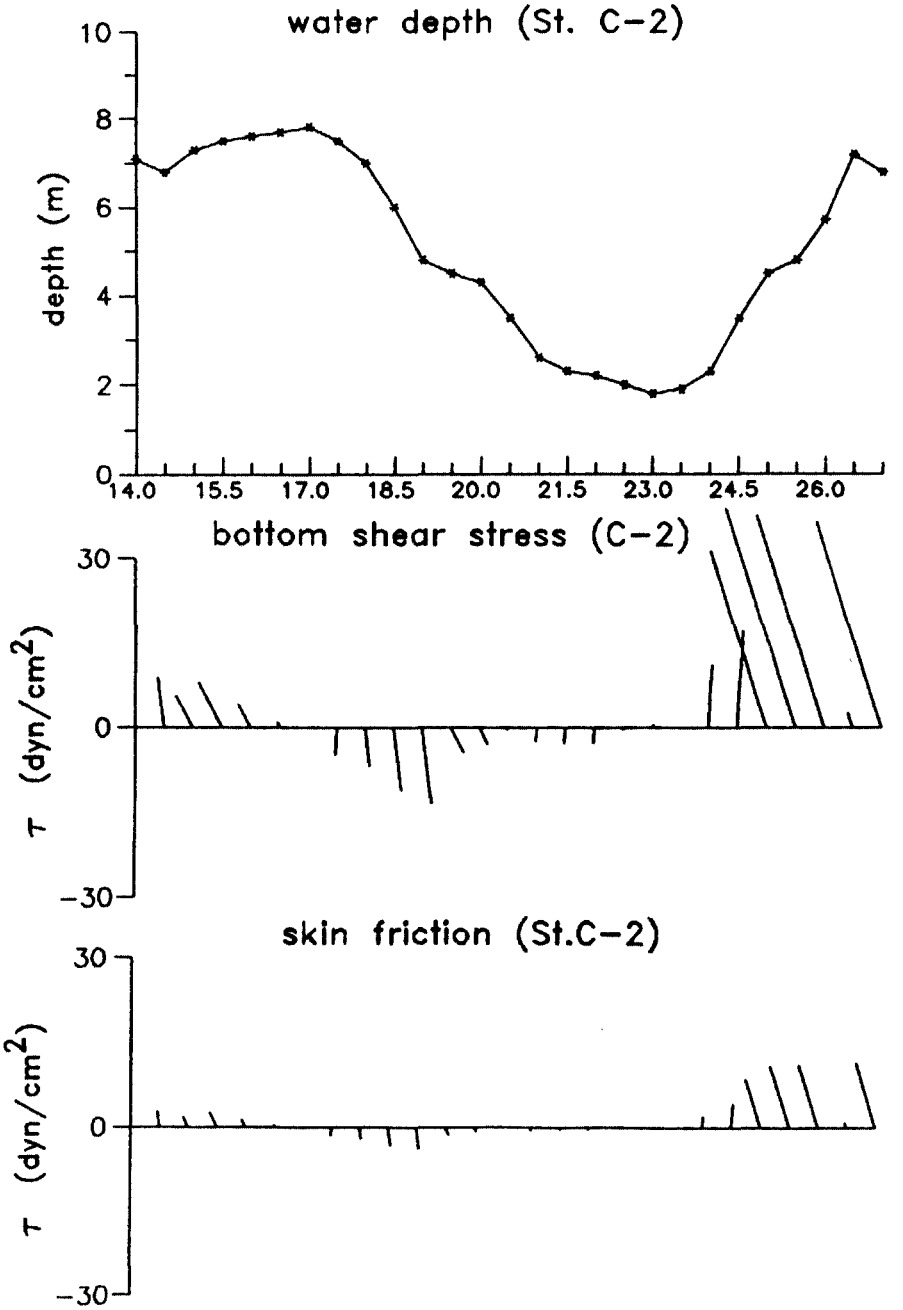

Figure 7. Bottom shear stress and skin friction in the south (C-3) during the spring tide.

may result in a net residual current on either side of the sand bar. Table 2 shows the residual currents at each station calculated by time-averaging the velocity components. The strongest residual current exists at the mid-depth at all stations, and it is stronger near the

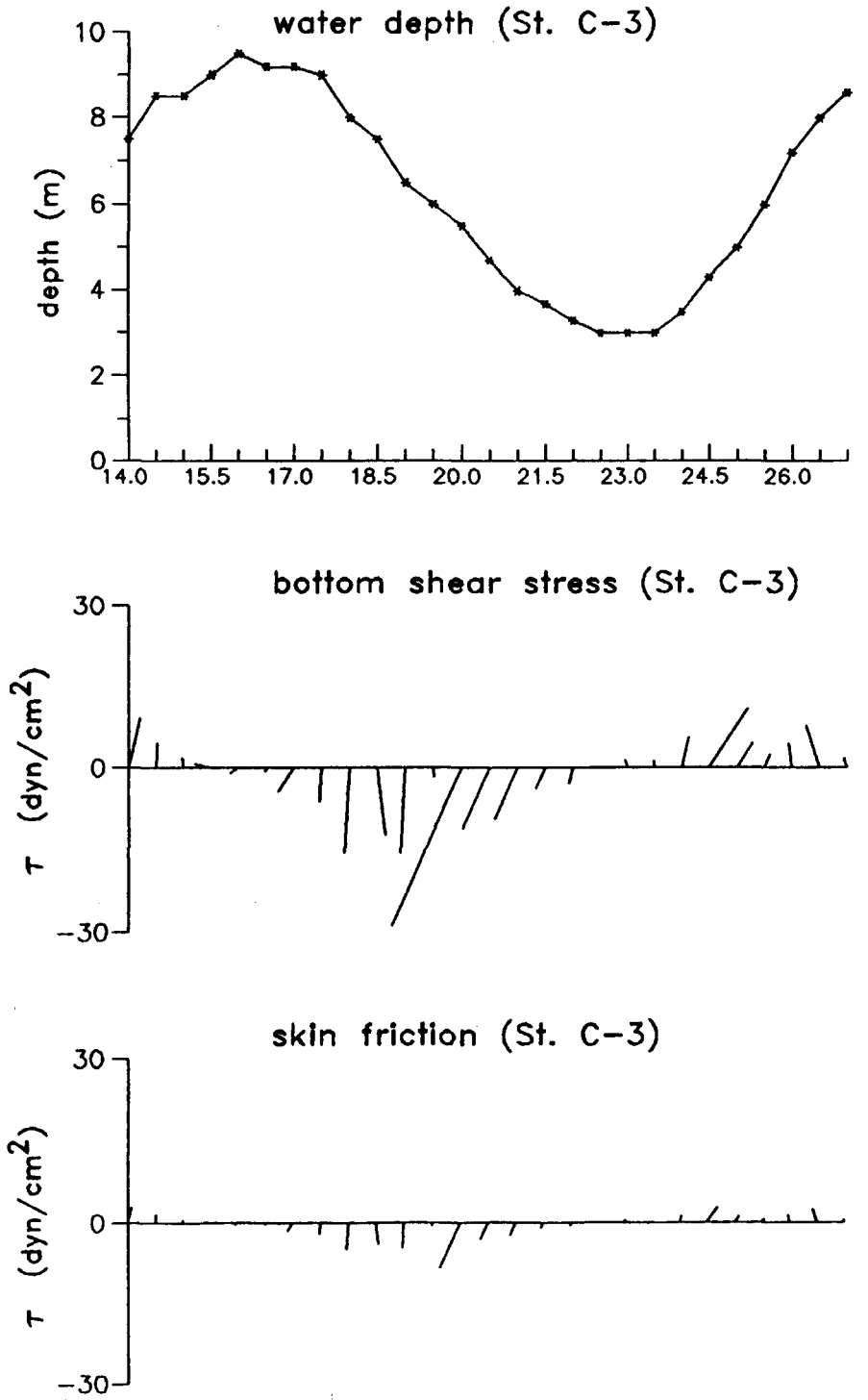

Figure 8. Bottom shear stress and skin friction in the north (C-3) during the spring tide.

bottom than the surface. Overall residual currents are stronger at the south than that at the north. The directions are NWW at the north and NEE at the south during the spring tide reflecting the tidal asymmetry at each station.

SEDIMENT MOVEMENT

When the acting shear stress on the grains near the bottom exceeds the critical shear stress to initiate the motion, the sediments are transported by the currents. The near bottom shear

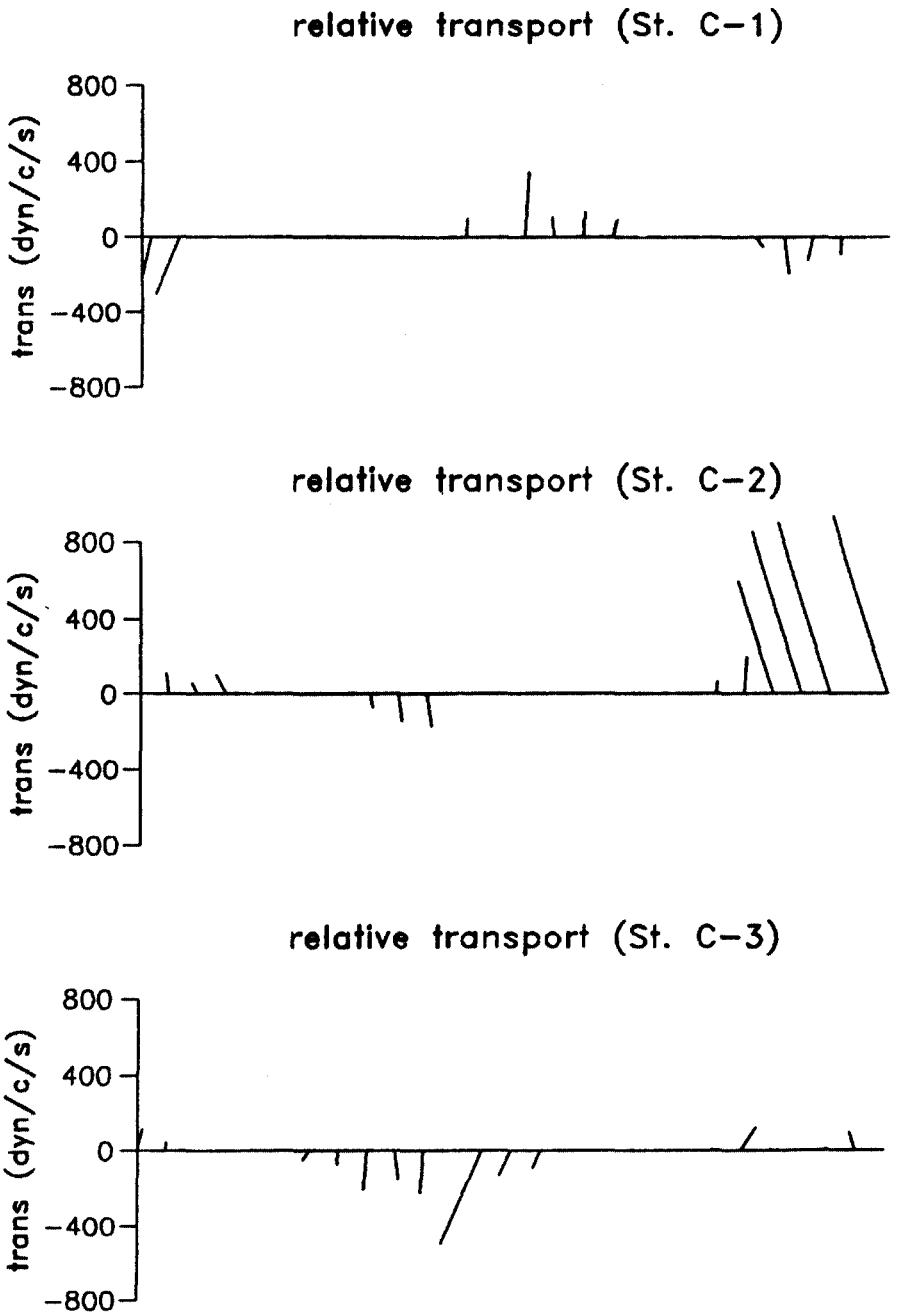

Figure 9. Relative rate of sediment transport at each station.

stress can be calculated by the quadratic stress law (Sternberg, 1972; McCave, 1973; Ludwick, 1975; Komar, 1976). However, the shear stress on a rippled surface may reflect the combined effect of skin friction and form drag (Einstein and Barbalossa, 1952; Vanoni and Hwang, 1967). Since the movement of surface sediment is only affected by the skin friction, the effect of form drag by the ripples should be removed from the calculated shear stress (Vanoni and Hwang, 1976).

Figures 6, 7, and 8 show the water depth and the calculated bottom shear stress and skin friction. It is suggested that the form drag is much larger than the skin friction. Figure 6 shows that the skin friction during the average tide does not show a significant asymmetry between flood and ebb. However, asymmetry in the magnitude of skin friction is most evident in the Figures 7 and 8. During the spring tide skin friction associated with the flood current is stronger in the south (Fig. 7), whereas the skin friction associated with the ebb current is stronger in the north (Fig. 8).

While the skin friction exceeds the critical shear stress the sediment is transported (Shields, 1936). The rate of bedload transport can be calculated in terms of stream power using the energetics bedload equation of Bagnold (1963). Figure 9 shows the relative rate of sediment transport per unit path width. It is clearly seen that strong asymmetry in the rate of sediment transport rate is directly associated with the tidal asymmetry during the spring tide resulting in a net sediment transport in one direction. However the asymmetry is much reduced during the average tide.

RESULT AND DISCUSSIONS

In the study area, numerous sand bars associated with the strong tidal currents develop. Long axes of the sand bars are parallel to subparallel to the direction of main tidal currents. Ripple marks and megaripples occur on the flat top of the sand bars. The existence of sand bars and the lack of sand or silt in the suspended sediment suggest that the sandy bottom sediment in the area is mostly transported as bedload.

Tidal currents measured at a sand bar show an asymmetrical pattern between flood and ebb currents. The asymmetry is most evident for the maximum speed during the spring tide, which suggests that the tidal distortion due to the sand bars is greater, as the current speed becomes stronger. Abrupt decrease in vertical velocity associated with strong bottom also stress develops when the surface currents are strong. The tidal asymmetry on either side of the sand bar is different each other. At the south the tides are flood-dominant whereas the tides are ebb-dominant at the north. Moreover the degree of asymmetry at the south is larger than that at the north. The maximum flood current in the south is stronger than the maximum ebb current in the north, and the maximum ebb in the south is weakther than the maximum flood in the north. The difference in asymmetry pattern seems to be the result of the development of tidal channels on either side. The channel in the south of the sand bar is deep and connected directly to the open sea whereas the channel in the north is shallow and interrupted by the Kokunsan islands. Thus the sand bar seems to be more affected by the flood current than the ebb current, even though ebb current is more affective in th north and flood current is more affective in the south. The rugged V-shape outline of the sand bar in the south also seems to reflect the stronger effect of flood current butting into the sand bank or bar.

The magnitude asymmetry on either side of the sand bar results in a net sediment transport in one direction. The direction of net sand movement by the tidal asymmetry may be onshore in the south and offshore in the north. Thus a net counterclockwise movement of sand around the sand bar is expected. However, more sand may be transported onshore due to the stronger flood-dominance in the south than the ebb-dominance in the north, which may result in a net onshore migration of the sand bar.

REFERENCES

Bagnold, R.A., 1946. Motion of waves in shallow water. Interaction of waves and sand bottoms. Proc. Roy. Soc. Ser. A **187:** 1-15.

Bagnold, R.A., 1963. Mechanics of marine sedimentation, in The Sea (Hill, M.N. ed.), Wiley-Intersci., New York, **3,** 507-528.

Belderson, R.H., Johnson, M.A. and Kenyon, N.H., 1982. Bedforms, in Offshore Tidal Sands (Stride, A.H. ed.), Chapman and Hall, London, 25-57.

Caston, V.N.D., 1972, Linear sand banks in the southern North Sea. Sedimentol., **18,** 63-78.

Caston, G.F., 1981. Potential gain and loss of sand by some sand banks in the southern bight of the North Sea. Mar. Geol., **41:** 239-250.

Einstein, H.A. and Barbalossa, N., 1952. River channel roughness, Trans. ASCE, **117:** 1121-1146.

Holman, R.A. and Bowen, A.J., 1982. Bars, bumps, and holes: models for the generation of complex topography. Jour. Geophys. Res., **87:** 457-468.

Howarth, M.J., 1982. Tidal currents of continental shelf. in Offshore Tidal Sand (Stride, A.H. ed.), Chapman and Hall, London, 10-26.

Huthnance, J.M., 1973. Tidal current asymmetries over the Norfolk sandbanks. Est. Coast. Mar. Sci., **1,** 89-99.

Hydrographic Office of Korea, Nautical Chart No. 335, Kogunsankundo and Approaches.

Hydrographic Office of Korea, 1990. Tide Table, Vol. 1.

Jordan, G.F., 1962. Large submarine sand saves, Science, **136,** 839-848.

Komar, P.D., 1976. The transport of cohesionless sediments on continental shelves, in Marine Sediment Transport and Environmental Management (Stanley, D.J. and Swift, D.J.P. eds.), John Wiley & Sons, NY: 107-125.

Komar, P.D., 1978. Relative quantities of suspension versus bedload transport on beaches. Jour. Sed. Petrol., **48:** 921-932.

Lee, H.J. and Chough, S.K., 1989. Sediment distribution, dispersal and budget in the Yellow Sea. Mar. Geol., **87,** 195-205.

Ludwick, J.C., 1972. Migration of tidal sand waves in Chesapeaks Bay entrance, in Shelf Sediment Transport: Process and Pattern (Swift, D.J.P. et al., eds.), Dowden, Hutohinson and Ross: 377-410.

Ludwick, J.C., 1975. Tidal currents and zig-zag sand shoals in wide estuary entrance. Geol. Soc. Am. Bull., **85:** 717-726.

McCave, I.N., 1973. Sand waves in the North Sea off the coast of Holland. Mar. Geol., **10:** 199-225.

Off, T., 1963. Rhythmic linear sand bodies caused by tidal currents. Bull. Am. Ass. Petrl. Geol., **47,** 324-341.

Shields, A., 1936. Anwendung der sehnlichkeitsmechanik und der turbulentz forschung auf die geschiebebewegungMitt. Preuss. Versuchanst. Wesserbau Schiffbau, Berlin, 26.

Sleath, J.F., 1984. Sea Bed Mechanics. Wiley-Intersci., New York, 334 pp.

Sternberg, R.W., 1972. Predicting initial motion and bedload transport of sediment particles, in Schelf Sediment Transport: Process and Pattern (Swift, D.J.P. et al., eds.), Dowden, Hutchinson and Ross: 61-82.

Stride, A.H., Belderson, R.H., Keynon, N.H. and Johnson, M.A., 1982, Offshore tidal deposits: sand sheet and sand bank facies. in Offshore Tidal Sands (Stride, A.H. ed.), Chapman and Hall, London, 95-124.

Vanoni, V.A. and Hwang, L.S., 1967. Relation between bed forms and friction in streams. Jour. Hydraul. Div., ASCE, 93, No. HY3: 121-144.

Received: November 10, 1991
Accepted: December 5, 1991